Tikrit Journal of Engineering Sciences (2025); 32(4): 2468
DOI: http://doi.org/10.25130/tjes.32.4.38

IRAQI Academic Scientific Journals

ISSN: 1813-162X (Print); 2312-7589 (Online)
Tikrit Journal of Engineering Sciences
available online at: http://www.tj-es.com

TJES Tikrit Journal of Engineering Sciences

Simulation and Experimental Validation of Stress Analysis for Train Coupler

Makmuri Nuramin [a,e], Anwar [a], Rohadi S. B. Utomo [*a], Djoko W. Karmiadji [a,b], Budi Haryanto [a,c], Yudi Irawadi [a], Budi Prasetiyo [a], Akhmad Sarif [a], Arga A. Nugroho [a], Muchamad Gozali [a], Indra H. Mulyowardono [a], Muhammad Awwaluddin [a,e], Hedi Purnomo [d]

a Research Center for Strength Technology of Structures, National Agency for the Research and Innovation, Puspiptek 15314, South Tangerang, Indonesia.
b Department of Mechanical Engineering, Pancasila University, Jakarta 12640, Indonesia.
c Mechanical Engineering Department, Engineering Faculty, University of Indonesia, Depok, Indonesia.
d The Indonesian Railroad Industry (INKA), Madiun 63122, East Java, Indonesia.
e Department of Industry Technology, Pamulang University, Banten 15418, Indonesia.

Keywords:
AAR Coupler; FEM analyses; Railway transportation; Strain gauge; Stress and load.

Highlights:

- Investigates stress distribution in a sand-cast steel train coupler using experiments and FEM simulation.
- Experimental stresses were higher than the simulated ones, with a <10% difference.
- Deviations attributed to casting defects, geometric irregularities, and material property variations.

ARTICLE INFO

Article history:

Received	06 Jan. 2025
Received in revised form	10 Apr. 2025
Accepted	15 May 2025
Final Proofreading	24 Oct. 2025
Available online	05 Dec. 2025

Citation: Nuramin M, Anwar, Utomo RSB, Karmiadji DW, Haryanto B, Irawadi Y, Prasetiyo B, Sarif A, Nugroho AA, Gozali M, Mulyowardono IH, Awwaluddin M, Purnomo H. **Simulation and Experimental Validation of Stress Analysis for Train Coupler**. *Tikrit Journal of Engineering Sciences* 2025; **32**(Sp1): 2468.
http://doi.org/10.25130/tjes.32.4.38

*Corresponding author:
Rohadi S. B. Utomo
Research Center for Strength Technology of Structures, National Agency for the Research and Innovation, Puspiptek 15314, South Tangerang, Indonesia.

Abstract: This study investigates the stress distribution in a sand-cast steel train coupler by comparing experimental results with FEM simulation. Strain gauges were attached to the coupler body areas to measure stresses under varying loads ranging from 500 kN to 1900 kN. The results indicated that the experimental and simulation stress values exhibited a linear relationship with increasing load, reaching a maximum of 206 MPa at 1900 kN. This stress value was approximately 30% of the material's yield strength. However, the experimental stress values tended to be slightly higher than the simulated results, with an average difference of less than 10%. This deviation is attributed to casting defects, geometric irregularities, and material-property differences that are difficult to capture in simulations. The specimen's chemical composition aligns with the Association of American Railroads (AAR) M201 Grade E Steel Casting standards, ensuring the material meets industry requirements. The findings suggest that optimizing the post-casting machining process could improve accuracy in future FEM analyses.

محاكاة والتحقق التجريبي من تحليل الإجهاد لرابط عربة القطار

مكموري نورامين[1,5]، أنور[1]، روهادي إس بي أوتومو[1]، دجوكو دبليو كارميادجي[1,2]، بودي هاريانتو[1,3]، يودي إيراوادي[1]، بودي براسيتيو[1]، أحمد صريف[1]، أرجا إيه نوجروهو[1]، موشاماد جوزالي[1]، إندرا إتش موليواردونو[1]، محمد أوال الدين[1,5]، هيدي بورنومو[4]

[1] مركز أبحاث تكنولوجيا قوة الهياكل/ الوكالة الوطنية للبحث والابتكار/ Puspiptek 15314/ جنوب تانجيرانج/ إندونيسيا.

[2] قسم الهندسة الميكانيكية/ جامعة بانكاسيلا/ جاكرتا 12640/ إندونيسيا.

[3] قسم الهندسة الميكانيكية/ كلية الهندسة/ جامعة إندونيسيا/ ديبوك/ إندونيسيا.

[4] صناعة السكك الحديدية الإندونيسية (INKA)/ مادیون 63122/ جاوة الشرقية/ إندونيسيا.

[5] قسم تكنولوجيا الصناعة/ جامعة بامولانج/ بانتن 15418/ إندونيسيا.

الخلاصة

تتناول هذه الدراسة توزيع الإجهاد في وصلة قطار فولاذية مصبوبة بالرمل بمقارنة النتائج العملية بمحاكاة طريقة العناصر المحددة. تم تثبيت مقاييس الإجهاد على مناطق جسم الوصلة لقياس الإجهادات تحت أحمال متباينة تتراوح بين ٥٠٠ كيلو نيوتن و١٩٠٠ كيلو نيوتن. أشارت النتائج إلى أن قيم الإجهاد العملية والمحاكاة أظهرت علاقة خطية مع زيادة الحمل، لتصل إلى حد أقصى بلغ ٢٠٦ ميجا باسكال عند حمل ١٩٠٠ كيلو نيوتن. وهذه القيمة للإجهاد تعادل حوالي ٣٠٪ من إجهاد الخضوع للمادة. ومع ذلك، اتجهت قيم الإجهاد العملية إلى أن تكون أعلى قليلاً من نتائج المحاكاة، بمتوسط فرق أقل من ١٠٪. ويعزى هذا الانحراف إلى عيوب الصب، وعدم الانتظام الهندسي، والاختلافات في خواص المادة التي يصعب محاكاتها بدقة. يتوافق التركيب الكيميائي للعينة مع معايير جمعية السكك الحديدية الأمريكية (AAR) للفولاذ المصبوب من الدرجة-M 201، مما يضمن مطابقة المادة لمتطلبات الصناعة. تشير النتائج إلى أن تحسين عملية التشغيل الآلي التي تلي الصب يمكن أن يحسن الدقة في تحليلات طريقة العناصر المحددة المستقبلية.

الكلمات الدالة: وصلة AAR؛ تحليلات طريقة العناصر المحددة؛ النقل بالسكك الحديدية؛ مقياس الإجهاد؛ الإجهاد والحمل.

1.INTRODUCTION

Most railway vehicle studies focus on the complete design process for the key structural components of the railway carriage, such as bogie frames, axles, wheels, and other components, including design procedures, assessment methods, verification, and manufacturing quality requirements [1]. In Indonesia, the technical specifications for a normal-speed train are regulated by the Ministry of Transportation Regulation Number PM 175 of 2015, which categorizes trains by propulsion type: namely, electric and diesel [2]. Railway transportation is one of the most widely used modes of transport in nearly every country, particularly in nations with large land areas. Its advantages include its effectiveness and efficiency in carrying people and goods, especially over long and medium distances. The component of rail transportation research is to experimentally observe the influence of actual loading factors on the prototype produced by the domestic manufacturing process [3, 4]. This issue underscores the crucial role of railway transportation worldwide. It highlights the need to enhance safety measures against train accidents and improve passenger security [5], such as material modifications, protective coatings for the train body, and the optimization of models and simulations [6-9]. Railway systems consist of various vehicles, including locomotives, self-propelled cars, and freight cars. During operation, these vehicles experience forces in the vertical (z-axis), lateral (y-axis), and longitudinal (x-axis) directions. Vertical forces are caused by dead loads (the weight of components installed on the vehicle) and live loads (the weight of passengers and/or cargo). Additionally, train wheel-rail and braking forces have a significant impact on the safety and reliability of the railway system [10-12]. Lateral forces, which are perpendicular to the track direction, are caused by track conditions such as track shifts, track inclination, and height differences, as well as environmental factors such as side wind pressure. Longitudinal forces result from locomotive tractive effort, braking, acceleration, and deceleration. Vertical forces are absorbed by the track in the vertical direction, lateral forces by the track in the lateral direction, and longitudinal forces by the coupler. Couplers connect locomotives with cars or freight cars and link cars or freight cars together. In addition to this function, a railway coupling also dissipates in-train forces, as previously mentioned [13]. Several couplers are commonly used in railway systems, including bar couplers, typically used on self-propelled cars, and AAR couplers, commonly used on locomotives and freight cars. AAR couplers have two sets, each including a coupler, knuckle, lock, and pin. During operation, the knuckles engage and lock together. The coupler, especially its head, receives the forces from the knuckle. AAR and bar couplers are manufactured using sand casting, followed by quenching and tempering. As a result, this gives the coupler better impact strength, though its surface is not as smooth as that produced by machining or rolling processes [14, 15]. Additionally, coupler systems must also address longitudinal discomfort, running instability, and vehicle disengagement [16-18], which can ultimately prevent failures in AAR Type E railroad couplers during application and enhance train and user safety [19, 20]. Therefore, it is necessary to test the stress analysis that occurs in this coupler. Stress analysis can be measured either experimentally using a strain gauge or through the Finite Element Method (FEM) using simulation software [21-23]. However, stress analysis using FEM simulations typically does not account for surface shape and roughness.

Therefore, based on the above description, this research aims to determine the accuracy of stress analysis results using FEM and validate them against actual stress analysis by directly measuring the stress on an AAR coupler produced through the sand casting process, which has a characteristic surface shape and roughness typical of cast products. The simulation software used is Ansys, while the experimental measurements are conducted using an LY 11-type electrical resistance strain gauge as the strain sensor. The results of this study are expected to provide data that can serve as a reference in the design and mass production of AAR couplers, offering reliable references for FEM-related simulations and other research.

2.EXPERIMENTAL CONSIDERATION OR SIDE

2.1.Materials and Methods

The specimen used in this study is AAR-M201 Grade E Steel Casting, as shown in Fig. 1, obtained from PT. Barata Indonesia, based on the AAR Manual of Standards and Recommended Practices for Couplers and Freight Car Draft Components, the sample is produced using the sand-casting method, with heat treatment and hardenability processes in accordance with AAR-M201 standards. The chemical composition of this sample is shown in Table 1. Then, the mechanical properties results, according to ASTM A370 for AAR-M201 Grade E steel casting, are presented in Table 2. Furthermore, to ensure the thickness of the test material used for comparison in the simulation design, the Olympus Epoch XT Panametrics NDT Ultrasonic Flaw Detector was used.

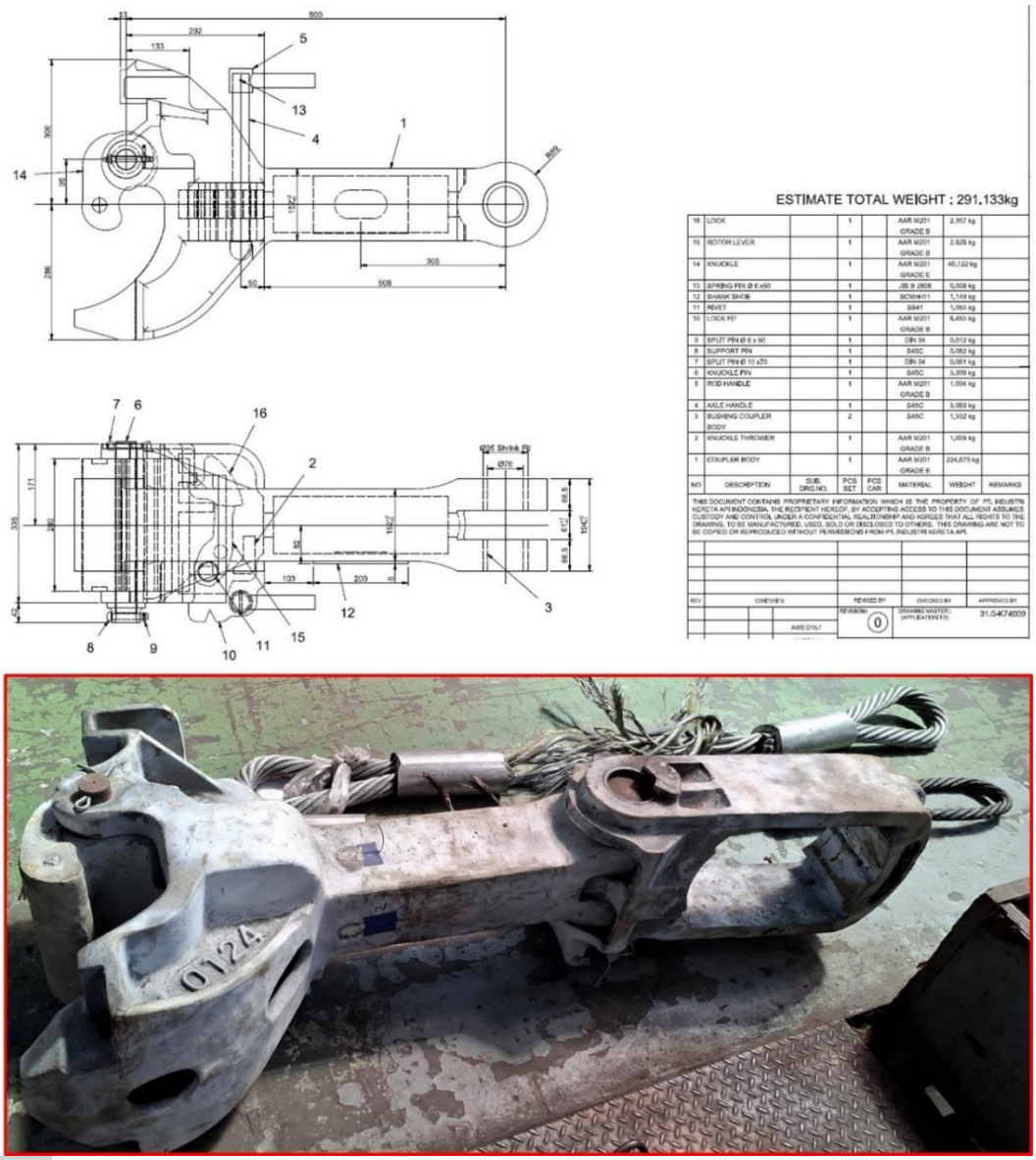

Fig. 1 Shape and Dimension of the AAR-M201 Type E Steel Casting Coupler from PT. Barata Indonesia.

Table 1 Chemical Composition of (the Association of American Railroads) AAR-M201 Grade E Steel Casting Material Samples by PT. Barata Indonesia [24].

Element	Weight (%)
C, max 0.32	0.282
Si, max 1.50	0.425
Mn, max 1.85	1.469
P, max 0.04	0.02
S. max 0.04	0.001
Cr	0.47
Mo	0.308
Cu	0.021
Ni	0.368
Al	0.077
Fe	Balance

Table 2 Mechanical Properties (the Association of American Railroads) AAR-M201 Grade E Steel Casting According to ASTM A370.

Element	Weight (%)
Tensile strength (MPa)	827
Yield point (MPa)	689
Elongation in 2", %	14
Reduction of area, %	30
Young's Modulus (MPa)	2×10^5
Poisson's Ratio (MPa)	0.3
density (kg/mm^3)	7.83×10^{-6}

2.2.The Simulation by ANSYS

In this study, simulations were performed using Ansys. The load variations applied were 500 kN, 600 kN, 700 kN, 800 kN, 900 kN, 1000 kN, 1100 kN, 1200 kN, 1300 kN, 1400 kN, 1500 kN, 1600 kN, 1700 kN, 1800 kN, and 1900 kN with the application at two locations corresponding to the experimental setup using strain gauges. The modeling used in this study is shown in Fig. 2. The modeling and simulation conditions are based on real-world applications in which the load-bearing area is the junction between the coupler and other components. The strain gauge locations were chosen because both areas are believed to be the most stable, thereby ensuring measurement accuracy. The simulation results showed the stress values in MPa at the two locations corresponding to the strain gauge, and a comparison will then be made between the experimental and simulation results.

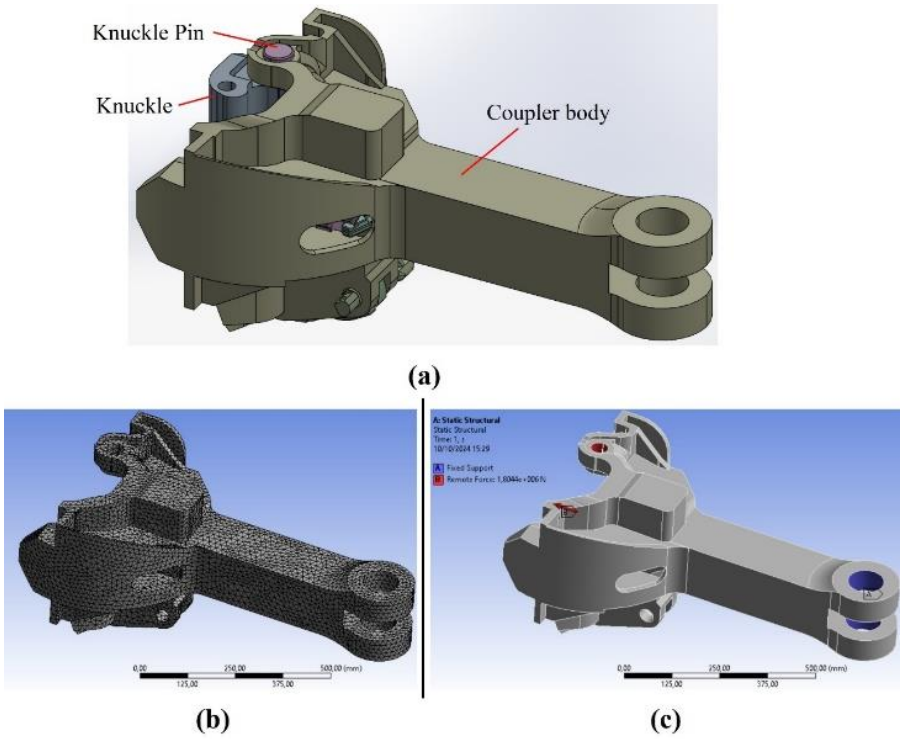

Fig. 2 (a) Modelling of Coupler Set with Knuckle, **(b)** Meshing of Coupler Model, and **(c)** Simulation Condition of Coupler Model.

2.3.Experimental Consideration

The experiment measured the strain at two points on the coupler using an LY 11-type electrical resistance strain gauge as the strain sensor. The strain gauge was mounted using the quarter-bridge method and connected to data-acquisition equipment to measure strain. The setup was configured to reflect actual conditions, where the load is applied when the knuckles engage. The coupler assembly was mounted horizontally on the test machine. The test machine used was a Schenck Trebel RHZ 4000 with a capacity of 4000 kN. The loading was applied incrementally to 1900 kN, ensuring that the resulting strain remained within the elastic limit of the material sample. During loading, force and strain data were recorded, and the results were compared with the simulation analysis. The strain gauge installation on the coupler, tested using the RHZ 4000 test machine, is shown in Fig. 3.

Fig. 3 Installation of Strain Gauges on Coupler Tested using RHZ 4000 Test Machine.

3.RESULTS AND DISCUSSION

The simulation results using Ansys program for the test material under loads of 500 kN, 600 kN, 700 kN, 800 kN, 900 kN, 1000 kN, 1100 kN, 1200 kN, 1300 kN, 1400 kN, 1500 kN, 1600 kN, 1700 kN, 1800 kN, and 1900 kN at two coupler locations can be seen in Fig. 4. From these results, it is evident that the selection of strain gauge locations on the sample is appropriate. These areas exhibit good material strength and stability because the load points are located at the junction between the coupler and other components. This stability is shown by the green color in the simulation model's test areas compared to other areas of the coupler.

Load: 500 kN

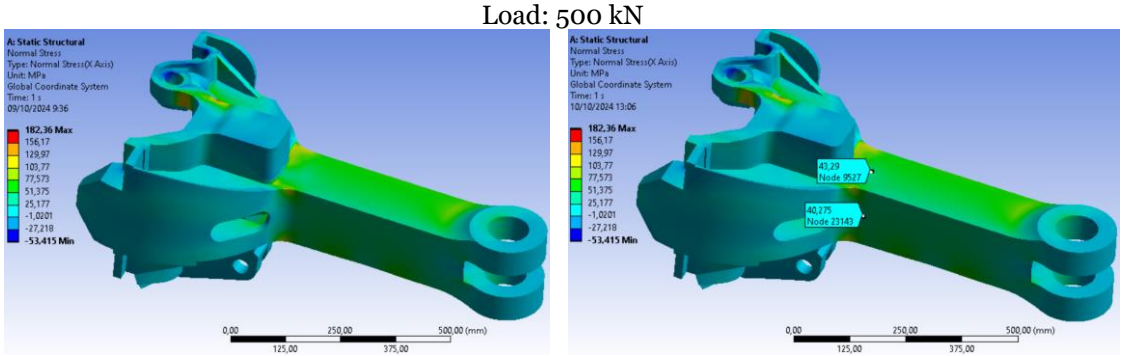

Load: 600 kN

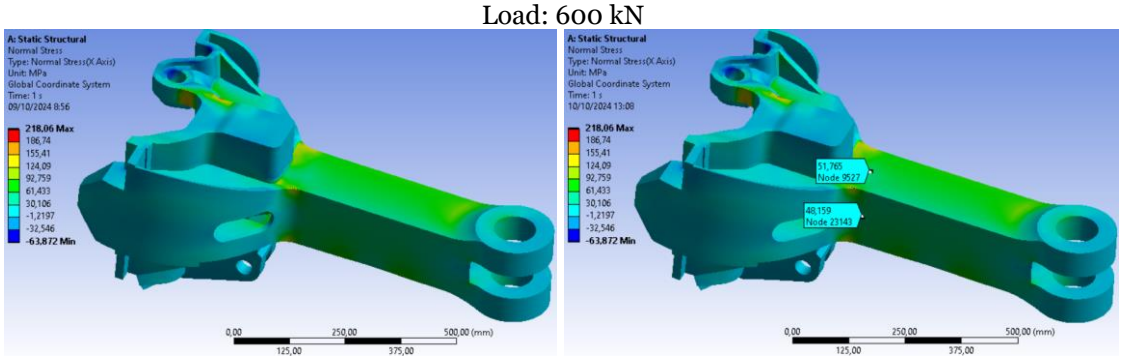

Load: 700 kN

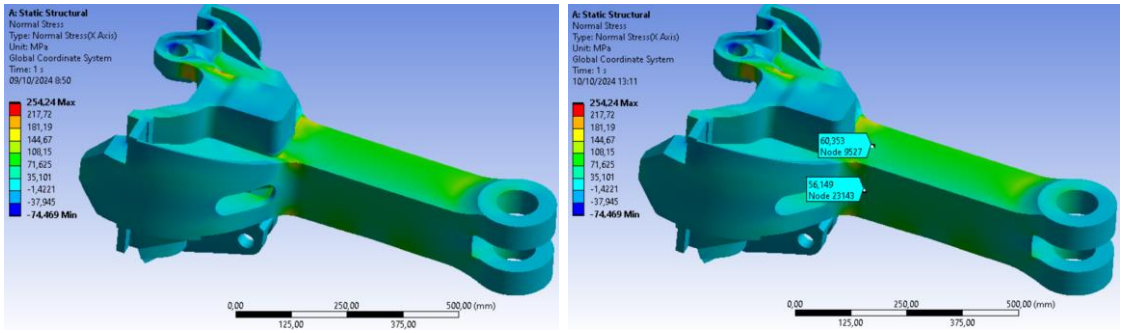

Load: 800 kN

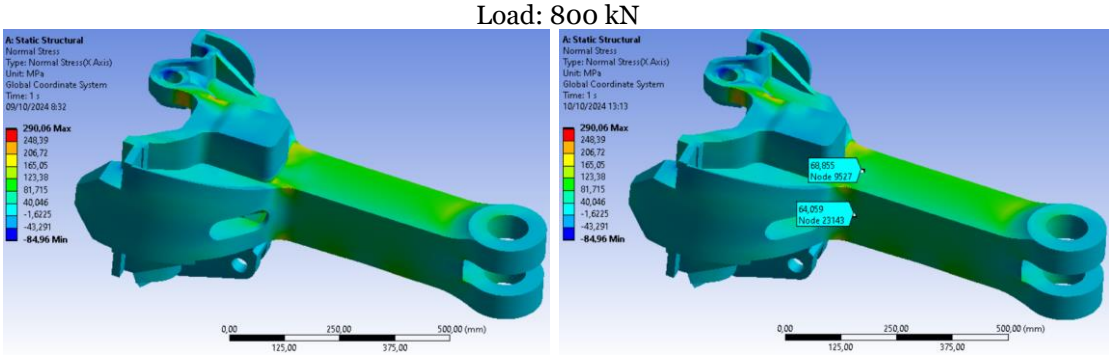

Load: 900 kN

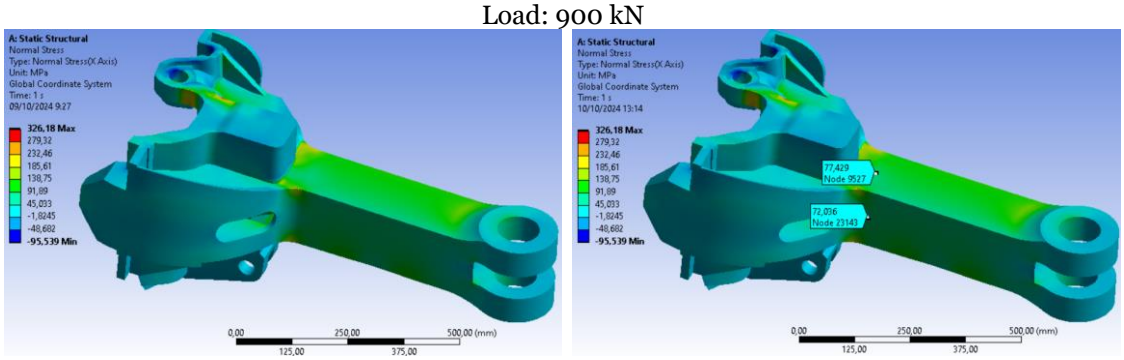

Load: 1000 kN

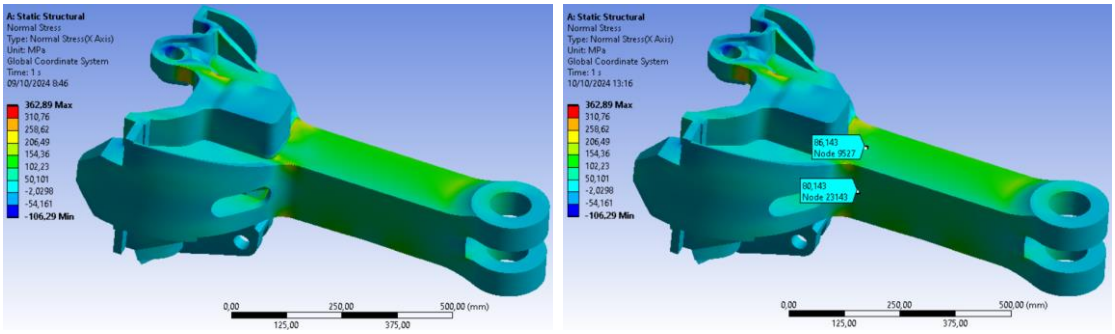

Load: 1100 kN

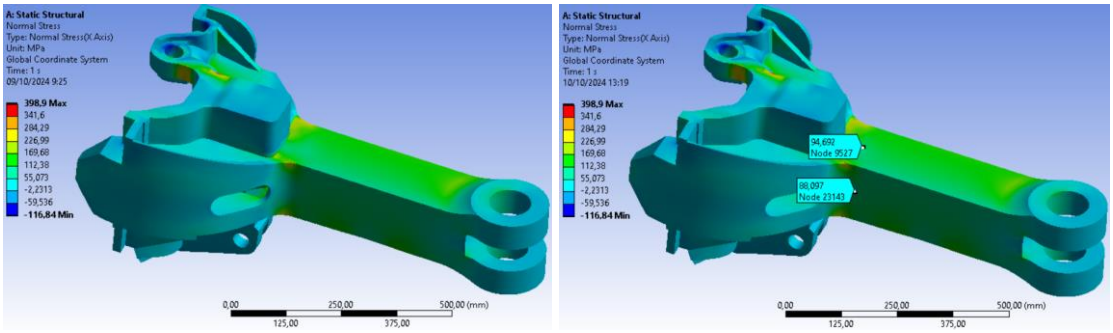

Load: 1200 kN

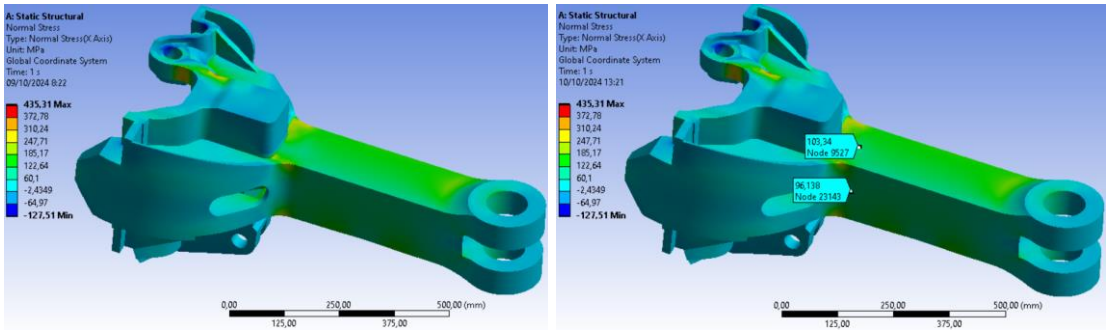

Load: 1300 kN

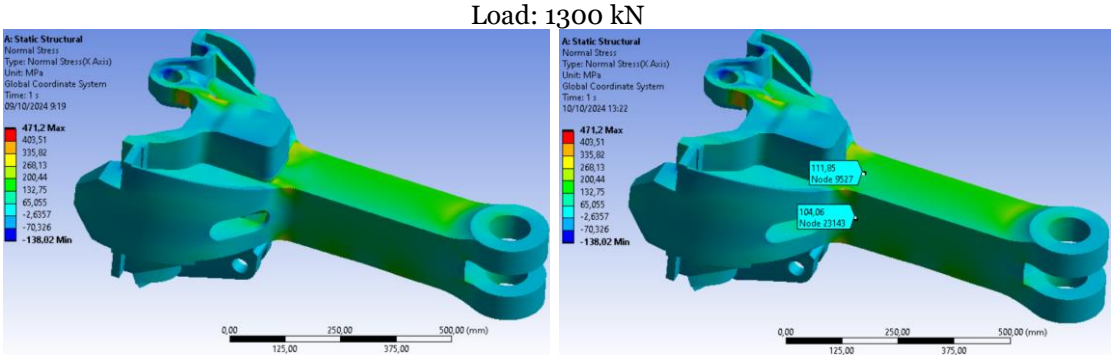

Load: 1400 kN

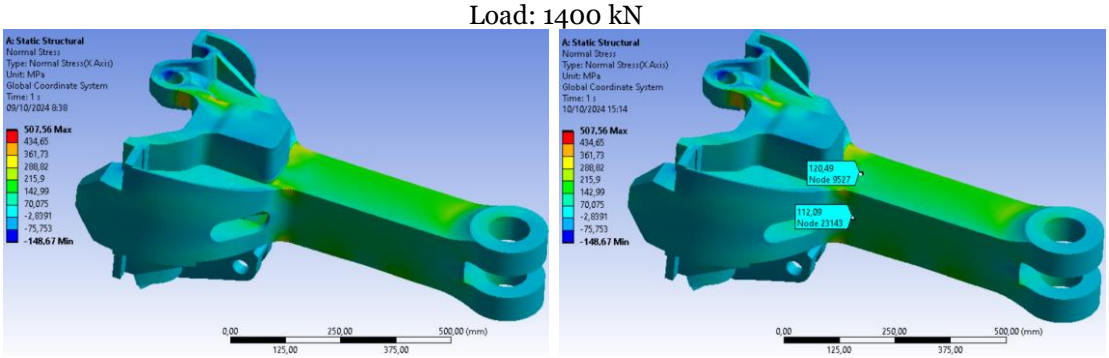

Load: 1500 kN

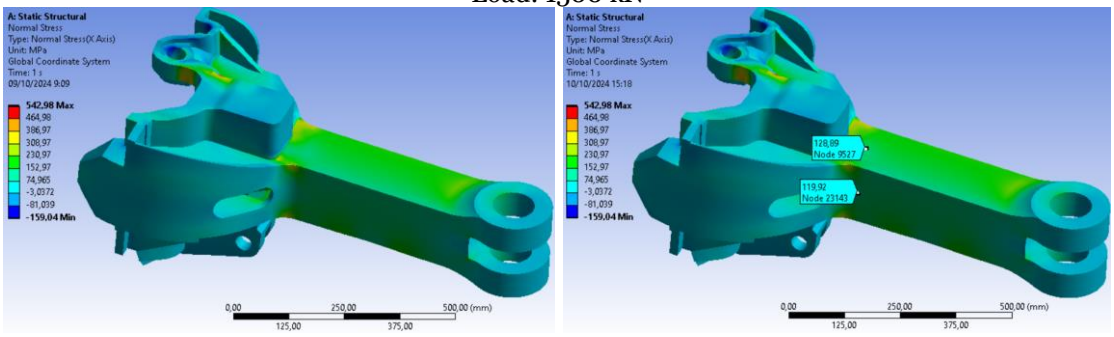

Load: 1600 kN

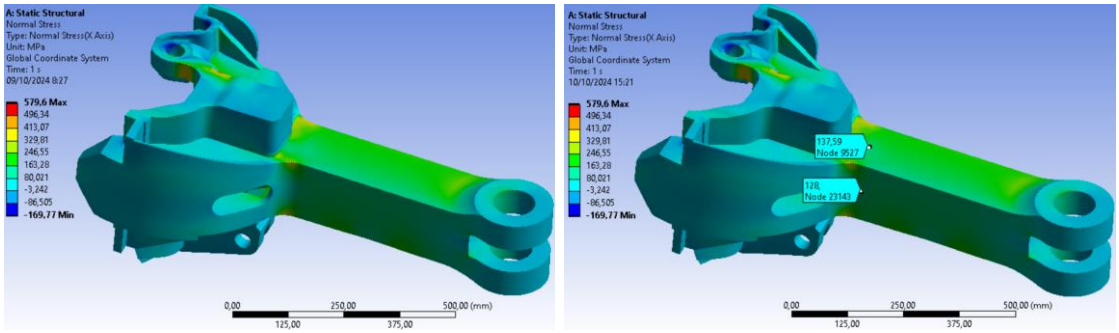

Load: 1700 kN

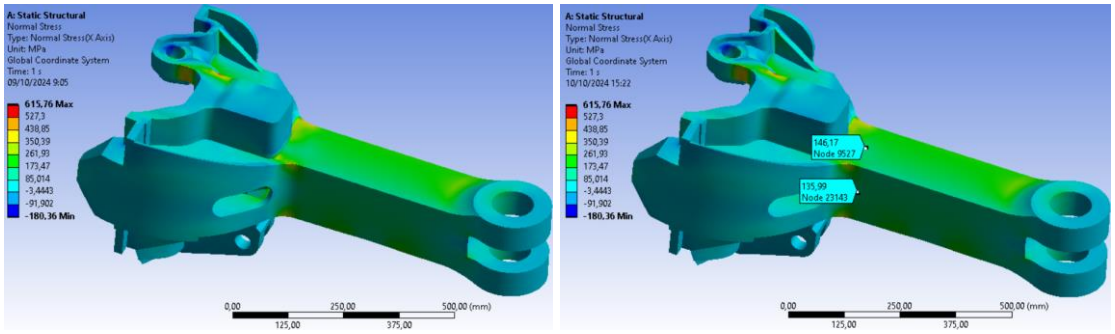

Load: 1800 kN

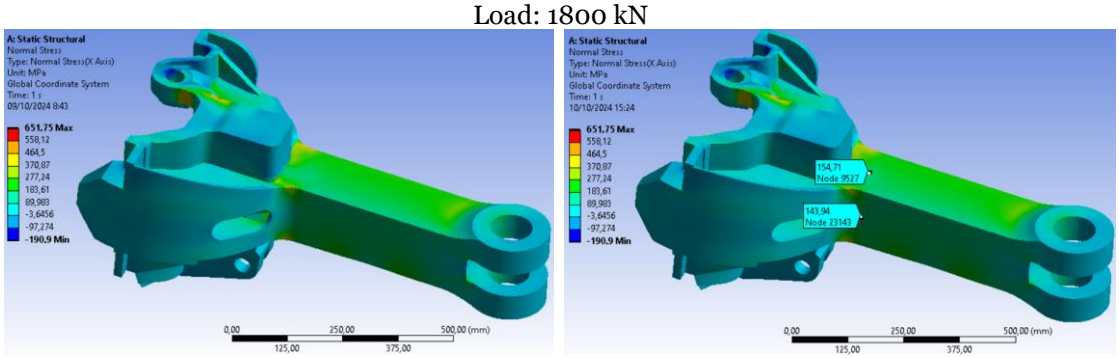

Load: 1900 kN

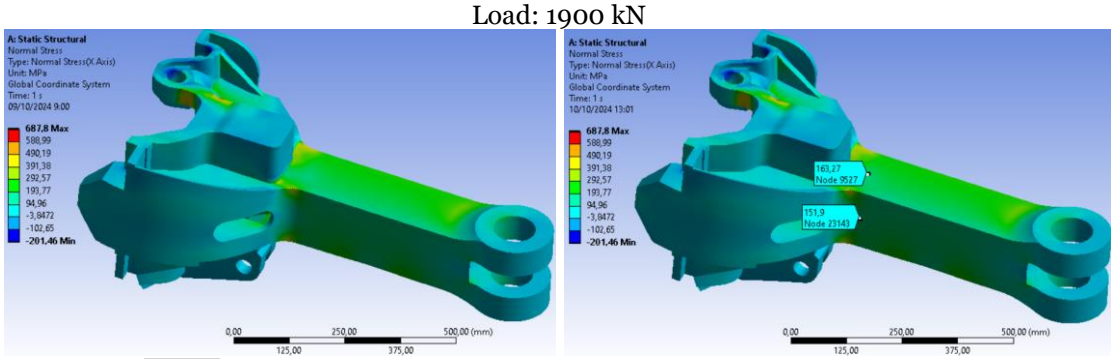

Fig. 4 Coupler Modeling for Simulation using Finite Element Method.

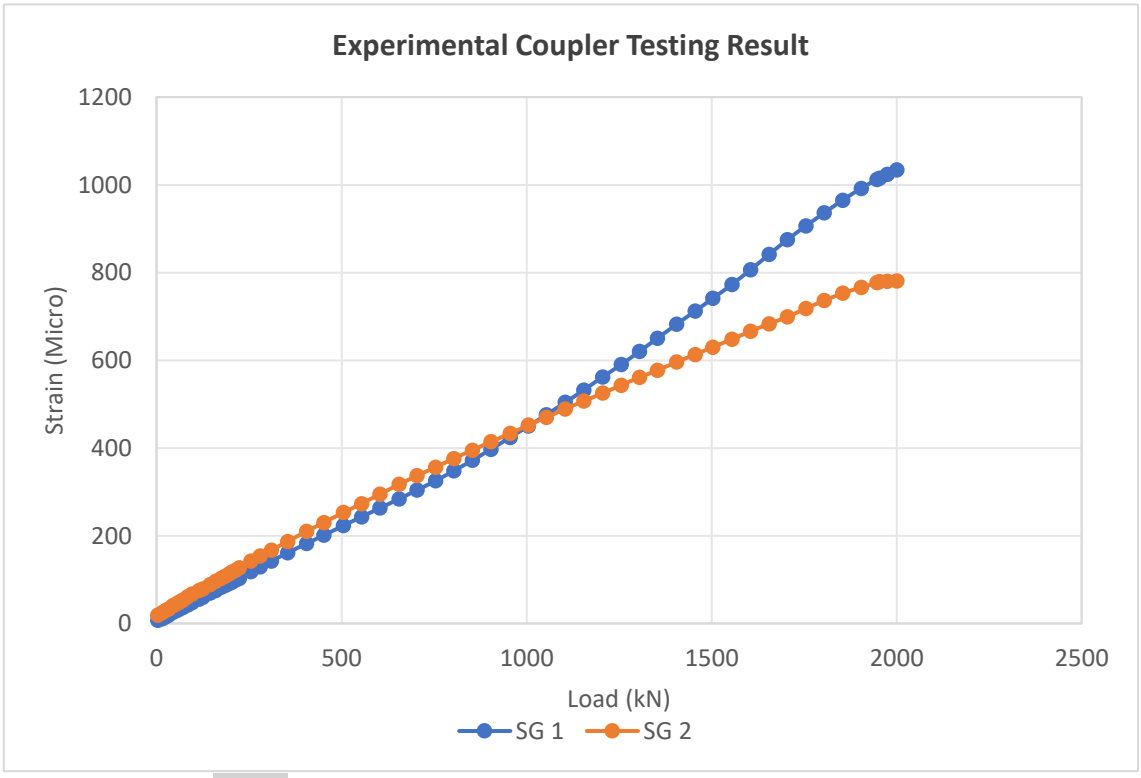

Fig. 5 Experimental Test Results of Strain Gauge in Coupler.

The experimental results for the coupler specimen are shown in Fig. 5, i.e., the blue line represents strain gauge 1, and the orange line represents strain gauge 2. The graph shows a linear relationship between the load (kN) and strain (microstrain) for the two strain gauges installed on the coupler. This result indicates that under loads less than 2000 kN, the strain remains within the elastic range, and the strain gauges and testing machine provide accurate data. Figure 5 also shows that the strain measured by strain gauge 1 was slightly higher than that measured by strain gauge 2. This behavior occurs because the load point is closer to strain gauge 1 than to strain gauge 2, as shown in simulations. To compare with the FEM simulation results, stress values were calculated at various loads. The stress values were determined using Hooke's Law: Stress = Strain × modulus of elasticity (E). According to the AAR Grade C material standard, E = 2×10^5 MPa. The stress values from the simulation and experimental testing, along with their differences at the various observed points, are shown in Tables 3 and 4. The comparison graphs of load (kN) versus stress (MPa) are shown in Fig. 6 for strain gauge 1 and in Fig. 7 for strain gauge 2. Table 3 shows that for the area under strain gauge 1, the lowest stress value at a load of 500 kN was 44.6 MPa for the experimental result and 43.29 MPa for the simulation, with a difference of 2.937%. Meanwhile, for the highest load applied in this study, 1900 kN, the stress at strain gauge 1 was 198.4 MPa in the experimental results and 163.27 MPa in the simulation analysis, resulting in a difference of 17.707%.

Table 3 Stress on The Coupler: Experimental Test and FEM Analysis for Strain Gauge.

No	Load (kN)	Experimental		Simulation (MPa)	% Difference
		Strain (SG1)	Stress (MPa)		
1	500	223	44.6	43.29	**2.937**
2	600	263	52.6	51.765	**1.587**
3	700	304	60.8	60.353	**0.735**
4	800	348	69.6	68.855	**1.07**
5	900	397	79.4	77.429	**2.482**
6	1000	450	90	86.143	**4.286**
7	1100	504	100.8	94.692	**6.06**
8	1200	562	112.4	103.34	**8.06**
9	1300	620	124	111.85	**9.798**
10	1400	682	136.4	120.49	**11.664**
11	1500	741	148.2	128.89	**13.03**
12	1600	806	161.2	137.59	**14.646**
13	1700	875	175	146.17	**16.474**
14	1800	936	187.2	154.71	**17.356**
15	1900	992	198.4	163.27	**17.707**
				Average	**8.526**

The load values chosen were aligned with real-world applications, where the applied load is typically less than 2000 kN. The lowest load displayed was 500 kN, which was chosen to properly adjust the strain gauge during testing to obtain more validated test data. The average percentage difference between the experimental and simulation results at strain gauge 1 was 8.562%. The smallest difference, 0.735%, occurred at 700 kN, while the largest difference occurred at 1900 kN. Figure 6 shows the Load-Stress graph for both the experimental and simulation results at strain gauge 1. The blue line shows the experimental results, while the red line shows the simulation analysis results. Both graphs exhibit a linear, constant increase with the applied load. It can also be observed that the simulation result is more linear than the experimental result. This behavior is expected, as the simulation analysis assumes standard, ideal, and unchanging conditions. On the other hand, the experimental results were heavily influenced by the quality and dimensions of the tested material, which in this case was a sand-cast steel specimen. The quality and dimensions of sand-cast steel depend on several factors, including the casting mold's quality, the steel's chemical composition, the casting technique, the mold design and gating system, the cooling and solidification process, and the post-casting treatment (heat treatment). Thus, while both the experimental and simulation results showed a linear increase in stress with increasing load, the difference between them was approximately 8.526%. Table 4 shows the experimental and simulation results for strain gauge 2. At this position, the lowest stress value at a load of 500 kN was 50.6 MPa for the experimental result and 40.275 MPa for the simulation analysis, resulting in a percentage difference of 20.405%, which is the largest percentage difference among the load variables tested in this study (500 kN – 1900 kN). Meanwhile, the stress value at the highest load in this study, 1900 kN, was 153.2 MPa for the experimental result and 151.9 MPa for the simulation analysis, with the smallest percentage difference among the load variables, at 0.849%.

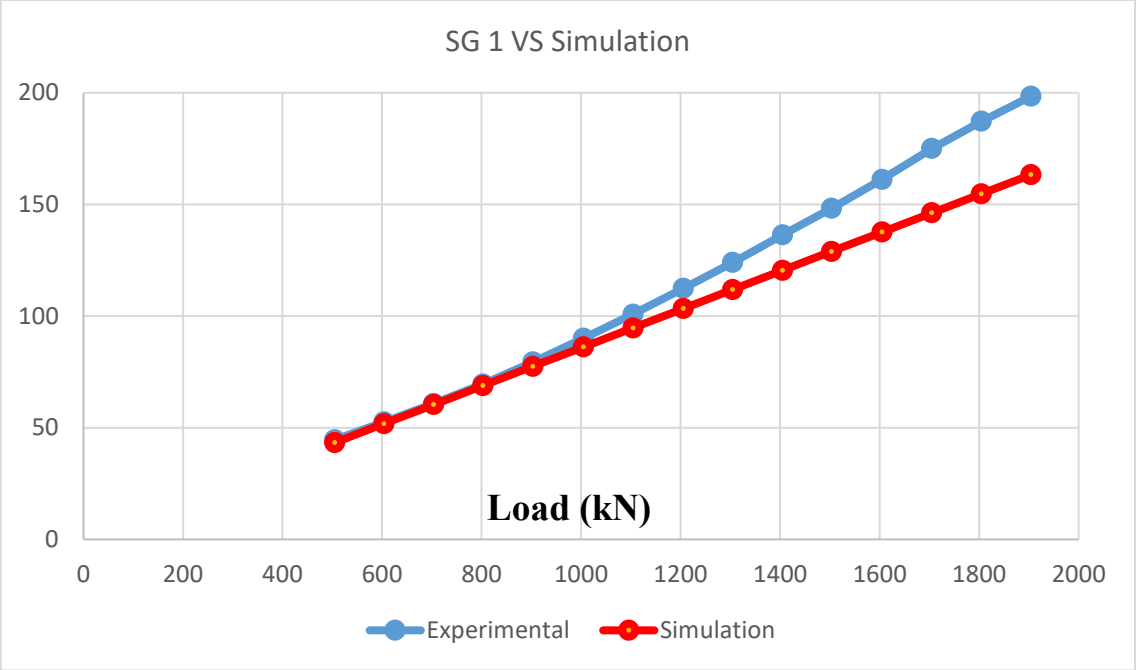

Fig. 6 Load and Stress Graph from Coupler at Strain Gauge 1.

Table 4 Stress on the Coupler: Experimental Test and FEM Analysis for strain gauge 2.

No	Load (kN)	Experimental		Simulation (MPa)	% Difference
		Strain (SG1)	Stress (MPa)		
1	500	253	50.6	40.275	**20.405**
2	600	295	59	48.159	**18.375**
3	700	337	67.4	56.149	**16.693**
4	800	376	75.2	64.059	**14.815**
5	900	414	82.8	72.036	**13**
6	1000	452	90.4	80.143	**11.346**
7	1100	489	97.8	88.097	**9.921**
8	1200	525	105	96.138	**8.44**
9	1300	561	112.2	104.06	**7.255**
10	1400	596	119.2	112.09	**5.965**
11	1500	630	126	119.92	**4.825**
12	1600	666	133.2	128	**3.904**
13	1700	699	139.8	135.99	**2.725**
14	1800	736	147.2	143.94	**2.215**
15	1900	766	153.2	151.9	**0.849**
				Average	**9.382**

Figure 7 shows the load-stress graph for both the experimental and simulation results at strain gauge 2. The stress values showed a linear response to the applied loads. The blue line represents the experimental results, while the red line shows the simulation results. Although there was a percentage difference between the two results, with an average of 9.382%, the simulation stress values were more linear and slightly lower than the experimental values at both strain gauge positions. This behavior occurred again because the simulation conditions were ideal, whereas the experimental results were obtained from actual sand-cast steel specimens, which can affect the experimental outcomes. It is important to note that several factors contribute to the more linear stress results in the load simulations than the experimental results for sand-cast steel. These factors include assumptions and simplifications in the simulation, variations in strain hardening and plasticity, the impact of defects on the experimental results, geometrical factors and boundary conditions, temperature effects, limitations of the simulation model, and the accuracy of experimental measurements. Several revalidations were performed based on the previously mentioned factors, such as checking the chemical composition in Sagita's study to validate the above results. The results can be seen in Table 1 and compared to the AAR-M201 Grade E Steel Casting standard, where the overall chemical composition of the test specimen aligns with the standards set by the AAR (Association of American Railroads). These findings reveal that the manufacturing process of a material can influence the accuracy of the FEM analysis conducted. In this study, the difference between the experimental and simulation results is less than 10%, indicating that, as previously mentioned, other factors may also contribute to this difference.

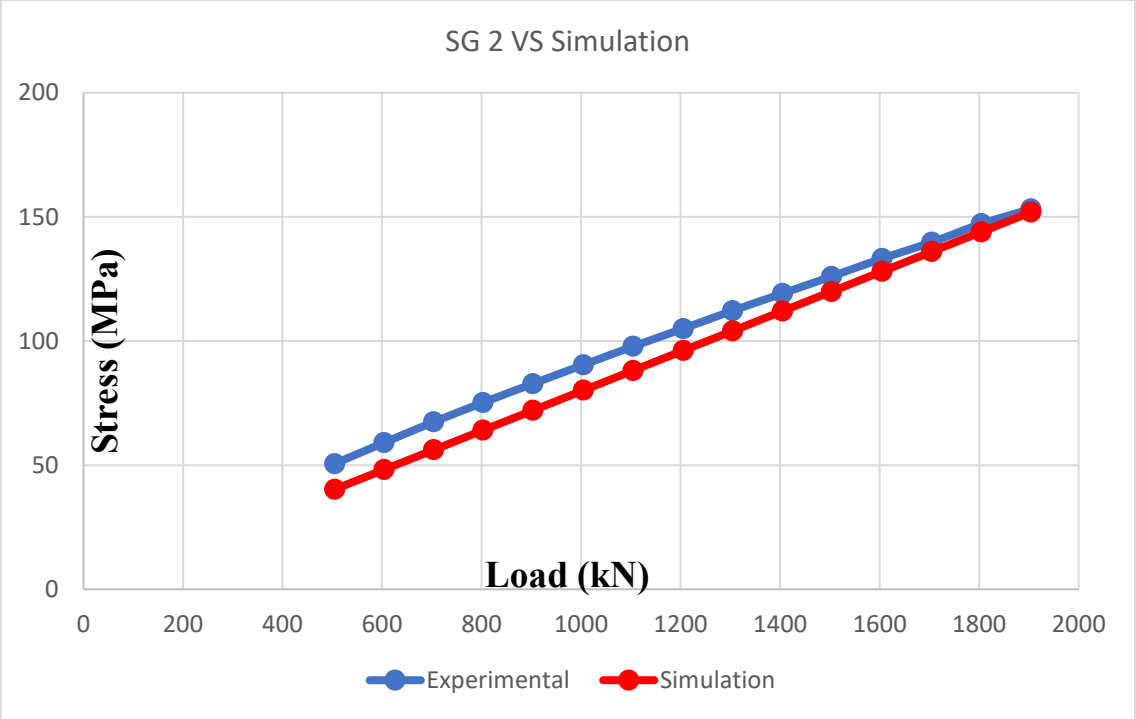

Fig. 7 Load and Stress Chart from Coupler at Strain Gauge 2.

4.CONCLUSIONS

The experimental and simulation results showed a linear relationship between the applied force and the measured stress, indicating that the specimen remained in the elastic region, i.e., remained strong, under the applied loads. The maximum stress at a load of 1900 kN in both strain gauge areas was 206 MPa, or 30% of the yield strength of the AAR material, ensuring that the specimen is very strong for real-world load applications. The difference between the experimental and simulation results showed that the experimental results tended to be higher, with the average percentage difference below 10%. Given that the chemical composition meets the standard and the simulation conditions are ideal, it suggests that other factors contribute to the accuracy difference between the experimental results and the FEM analysis of the coupler manufactured using the sand casting method. These parameters include the simulation assumptions and simplifications, strain hardening and plasticity variations, the impact of defects on the experimental results, geometrical factors and boundary conditions, temperature impacts, the simulation modeling limitations, and the experimental measurements' accuracy. The present study aimed to present the coupler's analysis results. In the future, it will be necessary to measure and analyze the coupler assembly, including the knuckle and pin, as these components bear heavy loads in a train assembly. Given the difference in accuracy between this study's experimental and simulation results, a key recommendation is to optimize the machining process after casting to better align the specimen's condition with the ideal.

REFERENCES

[1] Karmiadji DW, Haryanto B, Ivano O, Perkasa M, Farid AR. **Bogie Frame Structure Evaluation for Light-Rail Transit (LRT) Train: A Static Testing**. *Automotive Experiences* 2021; **4**(1): 36–43.

[2] Karmiadji DW, Gozali M, Anwar A, Purnomo H, Setiyo M, Junid R. **Evaluation of Operational Loading of the Light-Rail Transit (LRT) in Capital Region, Indonesia**. *Automotive Experiences* 2020; **3**(3): 104–114.

[3] Karmiadji DW, Haryanto B, Anwar, Prasetyo B, Irawadi Y, Farid AR, et al. **Verification of Urban Light Rail Transit (LRT) Bogie Frame Structure Design Lifetime under Variable Fatigue Loads**. *Mechanical Engineering for Society and Industry* 2022; **2**(1): 42–53.

[4] Haryanto B, Nuramin M, Karmiadji DW, Perkasa M, Anwar, Prasetiyo B, et al. **Verification of a New Prototype Design of Bogie Monorail Frame with Variation of Static Loading**. *Mechanical Engineering for Society and Industry* 2023; **3**(2): 78–85.

[5] Forsberg R, Björnstig U. **One Hundred Years of Railway Disasters and Recent Trends**. *Prehospital and Disaster Medicine* 2011; **26**(5): 367–373.

[6] Yu Y, Li J, Xie Z, Gao G, Rauf Sheikhi M, Li J. **Ballistic Performance of**

Aluminum Alloy Plates with Polyurea Coatings for High-Speed Train Structures. *Composite Structures* 2025; **351**: 118553.

[7] Gao J, Yuan R, Lin J, Lu S, Wang Y. **Thermal Response of High-Speed Train Multi-Layer Composite Floor Structure: Experimental and Numerical Analysis**. *Thermal Science and Engineering Progress* 2023; **46**: 102167.

[8] Hao Y, Jia L, Zio E, Wang Y, He Z. **A Network-Based Approach to Improving Robustness of a High-Speed Train by Structure Adjustment**. *Reliability Engineering and System Safety* 2024; **243**: 109857.

[9] Li T, Peng Y, Qiao Y, Zhu W, Zhang J, Wang K, et al. **Experimental Study on Crashworthiness and Lightweight of Cutting-Type Energy-Absorbing Structure of Magnesium Alloy for Trains**. *Engineering Structures* 2024; **301**: 117287.

[10] Guo F, He J. **Optimal Allocation Method of Electric/Air Braking Force of High-Speed Train Considering Axle Load Transfer**. *High-Speed Railway* 2024; **2**(2): 77–84.

[11] Zhang C, Yu Z, Jia L. **Train Wheel-Rail Force Collaborative Calibration Based on GNN-LSTM**. *High-Speed Railway* 2024; **2**(2): 85–91.

[12] Li J, Wang L, Wang X, Hu Z, Lan H, Wang Z, et al. **Effect of Shot Peening Equivalent Impact Force on Fatigue Crack Growth Behavior and Fatigue Life Prediction of Train Brake Discs**. *Engineering Failure Analysis* 2024; **166**: 108914.

[13] Yadav OP, Vyas NS. **The Influence of AAR Coupler Features on Estimation of In-Train Forces**. *Railway Engineering Science* 2023; **31**(3): 233–251.

[14] Xu J, Kang J, Mao W. **Effect of Double-Layer-Shell Sand Mold on the Residual Stress of Casting and Itself Crack Tendency**. *Materials Letters* 2023; **335**: 133752.

[15] Liu B, Kang J, Yang X, Zhang B, Bian Y. **Effects of Hollow Sand Mold on the Microstructure and Mechanical Properties of a Low Pressure Aluminum Alloy Casting**. *Journal of Materials Research and Technology* 2024; **28**: 4488–4497.

[16] Powell JP, Palacín R. **Passenger Stability Within Moving Railway Vehicles: Limits on Maximum Longitudinal Acceleration**. *Urban Rail Transit* 2015; **1**(2): 95–103.

[17] Sharma SK, Chaturvedi S. **Jerk Analysis in Rail Vehicle Dynamics**. *Perspectives in Science* 2016; **8**: 648–650.

[18] Vukšić Popović M, Tanasković J, Glišić D, Radović N, Franklin FJ. **Experimental and Numerical Research on the Failure of Railway Vehicles Coupling Links**. *Engineering Failure Analysis* 2021; **127**: 105497.

[19] Chunduru SP, Kim MJ, Mirman C. **Failure Analysis of Railroad Couplers of AAR Type E**. *Engineering Failure Analysis* 2011; **18**(1): 374–385.

[20] Li HF, Zhao XY, Yang SP, Wei JL, Gu XH, Liu YQ, et al. **Fatigue Failure Mechanism of High-Speed Train Bearing Steel after Long-Term Service**. *Engineering Failure Analysis* 2024; **165**: 108777.

[21] Chen Y, Jing L, Li T, Ling L, Wang K. **Numerical Study of Wheel–Rail Adhesion Performance of New-Concept High-Speed Trains with Aerodynamic Wings**. *Journal of Zhejiang University-SCIENCE A (Applied Physics & Engineering)* 2023; **24**(8): 673–691.

[22] Thejasree P, Dileep Kumar G, Leela Prasanna Lakshmi S. **Modelling and Analysis of Crankshaft for Passenger Car using ANSYS**. *Materials Today: Proceedings* 2017; **4**(10): 11292–11299.

[23] Milovanović V, Zivković M, Disić A, Rakić D, Zivković J. **Experimental and Numerical Strength Analysis of Wagon for Transporting Bulk Material**. *IMK-14 – Research & Developement in Heavy Machinery* 2014; **20**(4): 61–66.

[24] Sagita RN, Rochiem R, Wibisono AT. **Analisa Pengaruh Lama Waktu Tahan Tempering terhadap Struktur Mikro dan Sifat Mekanik Coupler Baja AAR-M201 Grade E**. *Jurnal Teknik Its Pomits* 2017; **16**(1): 35–40.